Biochemical Pharmacology 82 (2011) 1163–1174

Contents lists available at ScienceDirect

Biochemical Pharmacology

journal homepage: www.elsevier.com/locate/biochempharm

Direct inhibition of NF-κB activation by peptide targeting the NOA ubiquitin binding domain of NEMO

Jeanne Chiaravalli [a], Elisabeth Fontan [a], Hafida Fsihi [a], Yves-Marie Coic [b], Françoise Baleux [b], Michel Véron [a], Fabrice Agou [a,*]

[a] Institut Pasteur, Unité de Biochimie Structurale et Cellulaire, CNRS, URA 2185, France
[b] Institut Pasteur, Unité de Chimie des Biomolécules, CNRS URA 2128, 25/28 rue du Dr. Roux, 75724 Paris Cedex 15, France

ARTICLE INFO

Article history:
Received 19 May 2011
Accepted 15 July 2011
Available online 23 July 2011

Keywords:
IKK complex
NF-κB
Ubiquitin binding domain
Protein–protein interaction inhibitor
Ubiquitin linkage

ABSTRACT

Aberrant and constitutive NF-κB activation are frequently reported in numerous tumor types, making its inhibition an attractive target for the treatment of certain cancers. NEMO (NF-κB essential modulator) is the crucial component of the canonical NF-κB pathway that mediates IκB kinase (IKK) complex activation. IKK activation resides in the ability of the C-terminal domain of NEMO to properly dimerize and interact with linear and K63-linked polyubiquitin chains. Here, we have identified a new NEMO peptide inhibitor, termed UBI (ubiquitin binding inhibitor) that derives from the NOA/NUB/UBAN ubiquitin binding site located in the CC2-LZ domain of NEMO. UBI specifically inhibits the NF-κB pathway at the IKK level in different cell types stimulated by a variety of NF-κB signals. Circular dichroïsm and fluorescence studies showed that UBI exhibits an increased α-helix character and direct, good-affinity binding to the NOA-LZ region of NEMO. We also showed that UBI targets NEMO in cells but its mode of inhibition is completely different from the previously reported LZ peptide (herein denoted NOA-LZ). UBI does not promote dissociation of NEMO subunits in cells but impairs the interaction between the NOA UBD of NEMO and polyubiquitin chains. Importantly, we showed that UBI efficiently competes with the in vitro binding of K63-linked chains, but not with linear chains. The identification of this new NEMO inhibitor emphasizes the important contribution of K63-linked chains for IKK activation in NF-κB signaling and would provide a new tool for studying the complex role of NF-κB in inflammation and cancer.

1. Introduction

The nuclear factor-κB (NF-κB) proteins have essential roles in innate and adaptative immunity, oncogenesis, and development [1–4]. In resting cells, NF-κB transcription factors combined with inhibitors called IκB are inactive in the cytoplasm. The activity of NF-κB proteins is regulated by a variety of stimuli including bacterial lipopolysaccharides (LPS), tumor necrosis factor-α (TNF-α) and interleukin 1β (IL-1β). In the canonical pathway, stimulation leads to the activation of the IKK (IκB kinase) complex composed of two protein kinases (IKKα and IKKβ) and a non-catalytic regulatory protein called IKKγ/NF-κB essential modulator (NEMO). Once the IKK complex is active, the kinases phosphorylate IκB proteins which promote their K48-linked ubiquitination and proteasomal degradation, which subsequently allow NF-κB transcription factors to enter the nucleus and activate gene expression. Activation of the IKK complex relies on the interaction between the kinases and NEMO. NEMO interacts with many proteins that participate in a series of NF-κB activating signals.

Despite an abundance of literature on the IKK complex, the mechanism of its activation by NEMO remains confusing, probably because NEMO acts as an integrating platform for multiple signaling receptors. Nevertheless, a consensual mechanism has emerged. Genetic evidence supports the TGF-activated kinase (TAK1) as the direct upstream kinase for IKK in innate and adaptative immune responses [5,6]. Activation of TAK-1 depends on its interaction with K63-linked chains through its protein partners TAB2/TAB3, which specifically recognize these types of polyubiquitin chains [7,8]. Upon receptor activation, several signaling proteins such as receptor interacting protein 1 (RIP1) become K63-polyubiquitinated and promote recruitment of

Abbreviations: NF-κB, nuclear factor-κB; NEMO, NF-κB essential modulator; LZ, leucine zipper; CC2, coiled-coil 2; UBI, ubiquitin binding inhibitor derived from NEMO; NOA, NEMO Optineurin ABIN; CPP, cell permeable peptide; BA-peptide, peptide fused at its N-terminus with the cell permeable sequence antennapedia and conjugated with the bodipy fluorophore; A-peptide, Antennapedia tagged peptide; R_7- or R_9-peptide, peptide fused at its N-terminus with a hepta- or nona-arginine sequence; DDM, dodecyl maltoside; PBS, phosphate-buffered saline; LPS, lipopolysaccharide; PMA, phorbol 12-myristate 13-acetate; IL-1β, interleukine 1β; TNF-α, tumor necrosis factor α; UBD, ubiquitin binding domain.

* Corresponding author at: Unité de Biochimie Structurale et Cellulaire, Institut Pasteur, 25 rue du Dr. Roux, 75724 Paris Cedex 15, France. Tel.: +33 1 44 38 95 69; fax: +33 1 45 68 83 99.
E-mail address: fabrice.agou@pasteur.fr (F. Agou).

0006-2952/$ – see front matter © 2011 Elsevier Inc. All rights reserved.
doi:10.1016/j.bcp.2011.07.083

NEMO/IKK complexes to the membrane through NEMO binding with the K63-linked polyubiquitin chains. In contrast with K48-linked polyubiquitin chains which target proteins for proteasome degradation, K63-linked polyubiquitin chains provide a docking site for both NEMO/IKK and TAK1/TAB2/TAB3 complexes. This facilitates the direct phosphorylation/activation of IKKα and IKKβ by TAK1. However, this model has been recently challenged by TNF-R1 signaling studies which show that head to tail linear polyubiquitin chains can also mediate IKK activation via the LUBAC complex containing HOIL-IL, HOIP [9] and more recently SHARPIN [10–12]. This and other E3 ubiquitin ligase complexes such as cIAP1/2 and TRAF2 are also recruited to the TNF-R1 in a TNF-α dependent manner and LUBAC recruitment requires cIAPs-generated polyubiquitin chains [13]. Replacement of the endogenous ubiquitin gene with sets of ubiquitin mutants also showed that the IL-1 pathway requires K63-linked polyubiquitin chains to mediate IKK activation [14]. The same studies also showed that the TNF-α pathway uses other sets of ubiquitination enzymes (E2 and E3) to form mixed polyubiquitin chains capable of activating IKK complex [14].

Although many signaling proteins become ubiquitinylated upon receptor activation, previous data indicate that free unanchored K63-linked and mixed polyubiquitin chains can activate IKK and TAK-1 complexes via the ubiquitin binding activities of NEMO and TAB2/TAB3, respectively [15]. The NEMO protein is comprised of a series of coiled-coils with variable intrinsic stability (Fig. 1A). The N-terminal half of the protein contains a large coiled-coil region (CC1) and a helical domain 1 (HLX1) which form the dimeric coiled-coil structure that is required for interaction with IKK kinases [16,17]. The central region of NEMO, denoted HLX2 (residues 196–248), acts as a binding site for the viral KSHV-derived vFLIP [18]. Analysis of the structural complex of NEMO with vFLIP revealed that HLX2 forms a parallel dimeric coiled-coil [18]. The C-terminal domain of NEMO, is comprised of a coiled-coil motif (CC2), a leucine zipper (LZ), and a zinc finger motif (ZF) at the extreme C terminus [19]. It is involved in signal recognition through its dimerization and polyubiquitin binding [19].

The LZ domain of NEMO contains a region of high homology which has been identified in four other proteins: optineurin and ABIN 1, 2, and 3 [20,21]. This region is named NOA (NEMO Optineurin ABIN), but is also referred to as NUB/UBAN [22,23]. The NOA region binds to K63-linked chains [24,25] and linear chains [26,27]. The NOA ubiquitin binding site itself can only interact weakly with K63-linked or linear chains and exhibits more efficient binding in the context of the full CC2-LZ domain [24,25]. Several crystal structures of the CC2-LZ domain alone [26,27], in complex with DARPin [19], or in complex with short diubiquitin of K63-linked chains [28] or linear chains [27] have been recently reported (Fig. 1B). All of these structures showed that the CC2-LZ domain forms an elongated coiled-coil dimer. Within the CC2-LZ domain, the NOA binding site is built on an unusual and unstable coiled-coil where a cluster of charged and aromatic residues forms the dimerization core. These structures can be used to precisely define the essential requirements for CC2-LZ

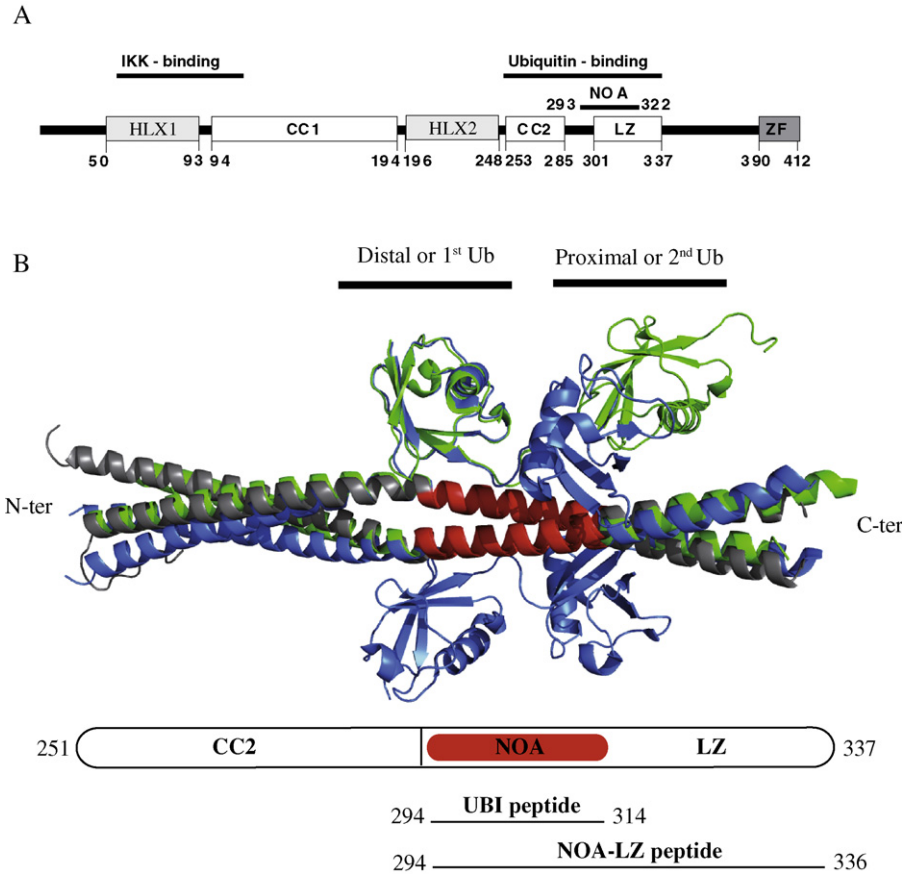

Fig. 1. The functional domains of the NEMO protein. (A) NEMO (412 amino acids in mouse) is composed of several overlapping functional domains: the IKK-binding domain, the minimal CC2-LZ oligomerization domain that is required for binding to K63-linked and linear ubiquitin chains, and the C-terminal ZF which represents a second UBD. Shown are the predicted coiled-coil regions (CC1, CC2, and LZ) and the ZF domains as well as the conserved NOA ubiquitin binding site. HLX1 and HLX2 refer to the two helical domains whose crystal structures showed that they also form coiled-coil structure [17,18]. (B) Superimposed structures of the CC2-LZ domain in complex with K63-linked (green, PDB ID: 3JSV) or linear diubiquitin chains (blue, PDB ID: 2ZV0), or with DARPin (grey, PDB ID: 2V4H). For clarity, the two bound DARPin molecules which overlap with the proximal Ub site of linear diubiquitin chain are not shown. The 21 amino-acid stretch of NEMO which constitutes the NOA is shown in red. It was used to design the UBI peptide. The NEMO-derived NOA-LZ peptide, previously reported as NF-κB inhibitor [20], is indicated below the structure.

dimerization and binding to linear and K63 diubiquitin (Fig. 1B). The structure of the C-terminal ZF domain of NEMO was also determined by NMR [29], which showed a second ubiquitin binding site [30]. This second site cooperates with the NOA motif to specifically recognize longer K63-linked chains [31].

Prolonged NF-κB activation and aberrant regulation of NF-κB are associated with many cancers and autoimmune disorders [32–34]. In this regard, NEMO is a promising therapeutic target for inhibitors because this protein is a central and non-redundant component of the IKK complex. Knockout of NEMO results in strong apoptosis of cancer cells in response to TNF-α via mechanisms which are dependent and independent of NF-κB transcription [35]. In addition, targeting NEMO may have less toxicity side effects in animal models compared with kinase inhibitors of IKK [32,36].

We have previously described a NEMO peptide termed LZ (hereafter denoted NOA-LZ), which inhibits the NF-κB pathway by perturbing the CC2-LZ oligomerization of NEMO [20]. More recently, we reported the NEMO-mediated mechanism of IKK activation in which the proper dimeric folding of NOA is required for efficient binding to polyubiquitin chains [19]. In this paper, we describe a new NEMO peptide derived from the NOA ubiquitin binding site. This peptide, termed ubiquitin binding inhibitor (UBI), is considerably shorter than the previously described NOA-LZ peptide and contains an Asp to Arg residue substitution at position 304. A mutation of the same Asp residue into Asn was found in a patient suffering from anhidrotic ectodermal dysplasia with immunodeficiency (EDA-ID) [37] and leads to NF-κB pathway inhibition by preventing NEMO interaction with polyubiquitin chains [25,27,38]. We show here that, contrary to the NOA-LZ peptide which inhibits NF-κB activation by perturbing dimerization of the CC2-LZ domain, the UBI acts as an NF-κB inhibitor by preferentially blocking interactions between K63-tetraubiquitin chains and the NOA UBD of the CC2-LZ domain of NEMO.

2. Materials and methods

2.1. Cell lines, plasmids and peptides

Jurkat T cells, 70Z/3, 70Z/3-C3, JM 4.5.2/Flag-NEMO cells were grown in RPMI 1640 medium (Invitrogen, Eugene, OR, USA) and HEK 293T cell lines were grown in DMEM medium (Invitrogen). Both media were supplemented with 10% FCS and 100 μg/ml penicillin/streptomycin. The stable cell line 70Z/3-C3 was obtained as described by Agou et al. [20]. The stable cell line JM 4.5.2/Flag-NEMO was obtained by electroporation of NEMO$^{-/-}$ Jurkat T lymphocytes (JM 4.5.2 [39]) with a pcDNA3-Flag-NEMO. AP-1-Luc and SRE-Luc plasmids were obtained from Stratagene (Santa Clara, CA, USA) and the Igκ-luc reporter plasmid for NF-κB has been previously described [26]. pNEMO-Flag was previously established by Fontan et al. [40]. The plasmids, pNFAT-luc and pGFP-NEMO were kind donations from J. Weitzman (CNRS/University Paris-Diderot) and A. Israël (Institut Pasteur, Paris), respectively. NF-κB reporter Jurkat T cells were either purchased from Invitrogen (NF-κB-bla Jurkat CellSensor cell line) or were obtained after transduction of lentiviruses containing a NF-κB reporter luciferase gene. For this, five tandem copies of an NF-κB binding site upstream of the TATA promoter and the firefly luciferase gene were cloned into a pLenti6.4/R4R2/V5-DEST vector (Gateway) from Invitrogen (sequence available upon request). The production of viral particles and infection of the cells were performed in accordance with the manufacturer's instructions using the ViraPower Lentiviral Expression System (Invitrogen). The peptides used in this study were all synthesized as previously described [41].

2.2. Cell stimulation assays

To test the activation of the NF-κB pathway, 70Z/3-C3 pre-B lymphocytes (4.5×10^5) in 450 μl of RPMI 1640 medium were incubated with 0–20 μM peptide. After 2 h at 37 °C, cell samples were transferred in duplicate to a 96-well microtiter plate (2×10^5 cells/well). Samples were then stimulated or not with 15 μg/ml LPS from Salmonella abortus (Sigma, St. Louis, MO, USA), or 20 ng/ml IL-1β (BD Pharmingen, San Jose, CA, USA), or 100 ng/ml PMA (Sigma) for 4 h at 37 °C. After centrifugation, the cell pellet was washed and cells were lysed in a 25 mM Tris-phosphate buffer pH 7.8 containing 8 mM $MgCl_2$, 1 mM DTT, 1% Triton X-100, 15% glycerol (LB buffer), and protease inhibitors (Roche Applied Science, Basel, Switzerland). β-Galactosidase activity was measured using the Galacton-star chemiluminescent substrate (Clontech, Madison, WI, USA) as previously described [20], and the β-lactamase activity of NF-κB-bla Jurkat cells (Invitrogen) was measured according to the manufacturer's instructions. To test the activation of different signaling pathways, Jurkat T cells were transiently transfected with an Igκ-luc, SRE-luc, NFAT-luc or AP1-luc reporter plasmid using a DEAE-dextran method as described by Courtois et al. [42]. All transient transfections were normalized with a second reporter plasmid bearing the β-galactosidase gene under the control of the EF1 constitutive promoter as described by Grubisha et al. [19]. 24 h after transfection, cells were incubated with or without 5 μM NEMO-derived peptides for 2 h. Cells were then stimulated or not with 100 ng/ml PMA and 1 μg/ml ionomycin for 5 h, and finally lysed in LB buffer. Measurement of luciferase was performed out in a Berthold Luminometer (Bad Wildbad, Germany).

2.3. Immunofluorescence confocal microscopy

70Z/3 cells were incubated with different peptides at 10 μM for 2 h at 37 °C and then were either stimulated or not with LPS (15 μg/ml) for 60 min. They were plated on poly-L-lysine-coated glass coverslips and fixed with 5% paraformaldehyde (20 min), washed in PBS, permeabilized with 0.2% Triton X-100, washed in PBS again, and blocked with 1% BSA for 15 min. Next, cells were incubated for 1 h at room temperature with a polyclonal anti-p65 antibody (gift from Nancy Reiss, diluted 1:1000 in blocking solution). Coverslips were washed 3 times with PBS and incubated with a 1:1000 dilution of the secondary antibody, Alexa-488 coupled goat anti-rabbit IgG (Invitrogen). They were washed and incubated with a 1:20,000 dilution of DAPI solution (Invitrogen). Finally, the samples were washed three times in PBS and mounted in mowiol for analysis on an Zeiss axioplan 2 microscope with ApoTome system for optical sectioning using the AxioVision 4.6.3 software (Chester, NJ, USA).

2.4. Fluorescence anisotropy and circular dichroism spectroscopy

Anisotropy measurements were performed with a Quantamaster fluorometer from Photon Technology International (Birmingham, NJ, USA) using a photomultiplier tube in the L-configuration as previously described [43]. All experiments were carried out in a microcuvette (60 μl) at 22 °C, with excitation and emission wavelengths of 495 and 513 nm in a 20 mM isoionic buffer pH 8 (10 mM acetic acid, 10 mM MES, 20 mM Tris, 20 mM KCl). Each data point is the result of 20 recordings taken over a 2-min period. Far-UV circular dichroism (CD) measurements were performed with an Aviv 215 spectropolarimeter (Lakewood, NJ, USA) as described by Grushiba et al. [19] with samples diluted in 10 mM sodium phosphate at pH 7.0.

2.5. Interaction of the UBI peptide with endogenous NEMO

70Z/3 cells were seeded in 6-well plates at a density of 10^6/ml in 2 ml aliquots and were incubated for 2 h at 37 °C with or without biotinylated BioA-NOA or BioA-UBI peptides. Cells were extensively washed two times with cold PBS to remove excess peptide and lysed in 100 μl of LB buffer containing protease inhibitors. Lysates were clarified at 13,000 × *g* at 4 °C for 20 min, and aliquots of 10 μl (10% of input) were withdrawn before incubating 40 μl of agarose high capacity neutravidin beads (Thermo scientific, Waltham, MA, USA) for 30 min at 4 °C with the remaining material. Biotinylated peptides were pulled down with beads and washed twice with LB buffer. Bound proteins and clarified lysates were then analyzed by Western blotting using anti-NEMO, anti-RIP (BD biosciences), anti-NRP (Cayman Chemicals, AnnArbor, MI, USA) or anti-GAPDH (Millipore, Billerica, MA, USA) antibodies.

2.6. In vivo NEMO oligomerization assay

HEK 293 T cells were transiently co-transfected with 2 μg pFlag-NEMO and 0.7 μg pGFP-NEMO by the calcium-phosphate-DNA precipitation method. The total amount of DNA was kept constant by adding empty vector. 24 h after transfection, cells were incubated with 20 μM of peptides for 2 h at 37 °C, washed twice with PBS and then lysed in 150 μl of LB buffer containing protease inhibitor cocktail. The Flag-NEMO/GFP-NEMO oligomers were pulled down by incubating for 1 h at 4 °C 100 μg of total protein in 200 μl of interaction buffer (50 mM Tris–HCl pH 7.5, 1% Triton X-100, 1 mM DTE, 300 mM NaCl) with 40 μl of agarose anti-Flag M2 beads (Sigma). The beads were washed twice with the interaction buffer and the GFP-NEMO fluorescence was directly read on the beads with a SAFAS microplate reader (Monaco). The clarified lysates were analyzed by Western blotting using anti-Flag (Sigma), anti-GFP (Oncogene, Cambridge, MA, USA), and anti-NDPK-B antibodies to normalize the results.

2.7. In vitro and in vivo ubiquitin binding assay

For in vitro experiments, the purified His-CC2-LZ (4 μM), which has been previously described [44], was bound to 50 μl of Ni-NTA beads (Qiagen, Hilden, Germany), equilibrated in 20 mM Tris–HCl buffer pH 8, 50 mM KCl, 0.2 mM DDM, 10% glycerol and 20 mM imidazole, for 30 min at room temperature. The beads were washed twice with the same buffer, incubated for 1 h with either K63- or linear tetraubiquitin (2 μM) and with 0-40 μM A-UBI and A-NOA peptides, and then washed twice. The sample was separated by SDS-PAGE and proteins were visualized by Coomassie blue staining of the gel. To determine the affinity of the labelled BA-NOA and BA-UBI peptides for K63-linked triubiquitin chains, fluorescence polarization measurements were taken in 50 mM Tris–HCl containing 150 mM NaCl at pH 7.5 using a concentration of peptide of 0.5 μM and a variable concentration of K63-linked triubiquitin chains. The normalized fractional binding was calculated as $(P_{obs} - P_{min}/P_{max} - P_{min}) \times 100$ where P_{obs} is the polarization signal at a given concentration of K63-linked triubiquitin, P_{min} is the polarization signal of the free peptide and P_{max} the polarization signal after saturation with K63-linked triubiquitin. Dissociation constants were calculated by fitting the experimental curve by nonlinear regression using the Hill equation for BA-NOA or the rectangular hyperbol equation for BA-UBI as described by Cordier et al. [30].

For experiments with cells, 24×10^7 JM 4.5.2 cells were stimulated or not with 10 ng/ml of TNF-α for 10 min at 37 °C, washed twice with cold PBS and lysed in 900 μl of LB buffer. 150 μl of proteins were incubated for 2 h at 4 °C with 150 μl of streptavidin magnetic beads (Novagen, Darmstadt, Germany) pre-incubated for 1 h at 4 °C with 10 μg of biotynilated-CC2-LZ with or without 20 μM of peptides. Beads were then washed four times in 10 mM Hepes pH 7.5, 150 mM NaCl, 8 mM $MgCl_2$, 10% glycerol, 0.1 mM DDM and 1 mM DTE and were resuspended in Laemmli buffer with 6 M urea. Polyubiquitin chains were detected by immunoblotting with an anti-ubiquitin antibody (Sigma).

2.8. IKK complex kinase assay

70Z/3 cells were plated at 5×10^6 cells/well, incubated with or without 10 μM A-UBI peptide for 2 h at 37 °C, stimulated for 45 min with 15 μg/ml LPS at 37 °C and lysed in 100 μl of LB buffer in the presence of protease and phosphatase inhibitors (Sigma). IκB kinase complexes were isolated from cell extracts by immunoprecipitation with anti-NEMO coated protein G beads (GE Healthcare) in TNT buffer (20 mM Tris–HCl pH 7.5, 200 mM NaCl, 1% Triton X-100). The beads were resuspended in kinase buffer (50 mM Tris–HCl pH 7.5, 500 mM NaCl, 10 mM $MgCl_2$, 5 mM $MnCl_2$, 2 mM DTE) containing 10 mM ATP, and protease and phosphatase inhibitors. GST-IκBα (residues 1–54) was added as a substrate for IKKβ for varying lengths of time. The sample was separated by SDS-PAGE and immunoblotted with a monoclonal phospho-IκBα antibody (Cell signaling, Beverly, MA, USA). The amount of IKKβ in each assay was determined with a mouse monoclonal anti-IKKβ antibody (Imgenex, San Diego, CA, USA).

3. Results

3.1. The UBI peptide, but not NOA, specifically inhibits the NF-κB pathway

The UBI peptide was chemically synthesized (residues 294–314 of mouse sequence) and differs from the NOA peptide by a single Asp to Arg substitution at position D304. Each of the two peptides studied (NOA and UBI) were fused at the N-terminus with several cell-permeable peptides (CPP) which were probed as internalization sequences. This comprised a 16-residue extension derived from the Antennapedia penetratin protein (A), hepta- and nona-arginine (R_7 and R_9), and the transactivator of transcription (TAT) sequence (see [45,46] for a review). All of the peptides used and CPP fusion sequences are described in Table S1. The BODIPY fluorophore (B) was conjugated at the N-terminus of the extended polypeptides. Cellular uptake of the BA-NOA, BA-UBI, BR_7-UBI, BR_9-UBI, and BTAT-UBI peptides was followed by FACS experiments. The internalization efficiency was the same for all fusion sequences tested (Table S2).

To analyze the effect of BA-NOA and BA-UBI on LPS-induced NF-κB activation, NF-κB reporter pre-B 70Z/3 lymphocytes (70Z/3-C3) were used as previously described [20]. A 50-fold increase in the NF-κB activity was observed after the 70Z/3-C3 cells were stimulated for 4 h with 15 μg/ml LPS. Incubation of cells with either BA-NOA or a longer NOA peptide had no effect on LPS-induced NF-κB activation. This longer peptide was denoted BA-NOA-LZ^{PP} (residues 294–336), and contained two Leu → Pro substitutions at positions 322 and 329 in the C-terminal half of NOA-LZ. In contrast, BA-UBI was a strong inhibitor with a calculated IC_{50} of 1.1 ± 0.1 μM (Fig. 2A). This corresponded to a 70% reduction of NF-κB activity at 10 μM. The IC_{50} value was similar for BR_7-UBI, BR_9-UBI and BTAT-UBI, indicating that the effect of this peptide was not linked to the CPP sequence (Table S2). The inhibitory activity of the unlabeled A-UBI was also compared with those of other NEMO and IKK-antagonistic peptides [20,67]. A-UBI was the most potent inhibitor with an IC_{50} value 11- and 21-fold lower than those of A-NOA-LZ and A-NBD peptides, respectively (Table S3). BA-UBI was also able to inhibit the IL-1β (20 ng/ml) or phorbol 12-myristate 13-acetate (PMA) (100 ng/ml) induced activation of NF-κB (Fig. S1). To

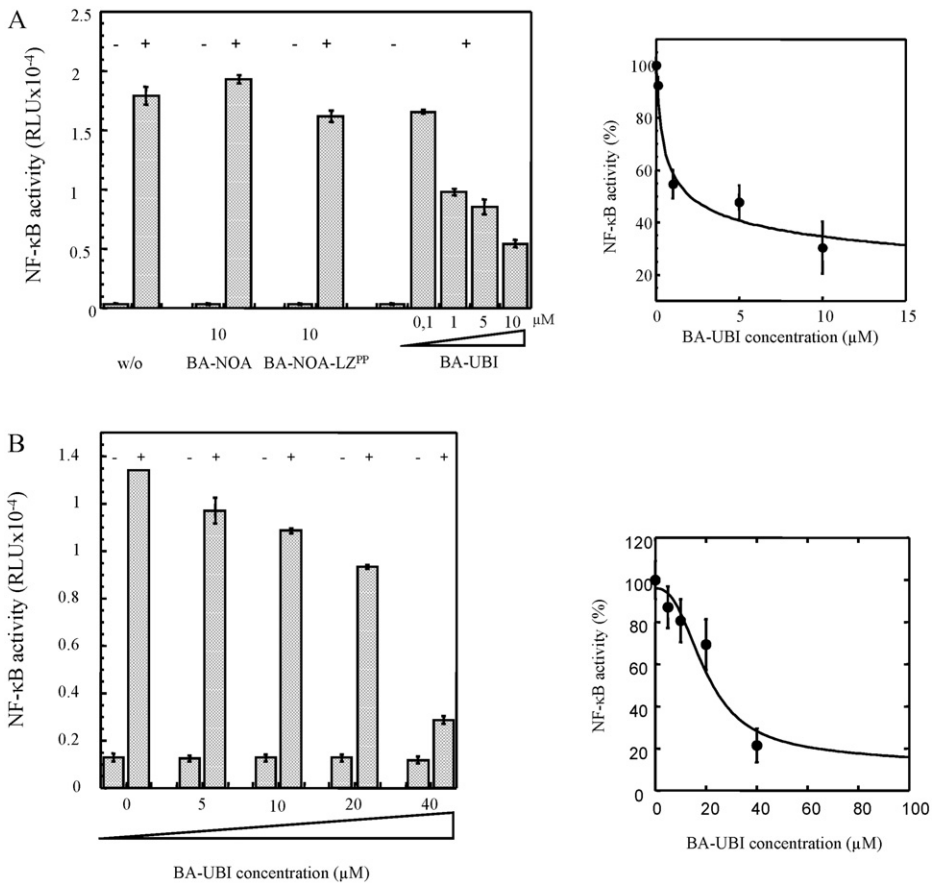

Fig. 2. Inhibition of NF-κB activation by UBI peptide. (A) NF-κB reporter pre-B lymphocytes 70Z/3-C3 were either left untreated (w/o) or treated for 2 h with an increasing concentration (0–10 μM) of BA-UBI, 10 μM BA-NOA, or 10 μM BA-NOA-LZ^{PP} before mock-stimulation (−) or stimulation (+) with LPS for 4 h. NF-κB activity was measured using the β-galactosidase assay. The mean values (±SD) from three separate experiments are shown. The right panel represents the inhibition curve of LPS-induced NF-κB activation by BA-UBI in pre-B lymphocytes leading to a calculated IC_{50} of 1 ± 0.1 μM. (B) Stably transduced NF-κB reporter T lymphocytes cells were treated for 2 h with an increasing concentration (0–40 μM) of BA-UBI, before stimulation with (+) or without (−) TNF-α for 4 h. NF-κB activity was measured using the luciferase assay. Mean values (±SD) from triplicate experiments are shown. RLU, relative light units. The right panel shows the inhibition curve of TNF-α induced NF-κB activation by BA-UBI, providing an IC_{50} value of 21 ± 4 μM.

investigate the effect of BA-UBI on TNF-α-induced NF-κB activation, another cell line expressing both TNF-receptors 1 and 2 was used. These cells were stably transduced with lentivirus bearing a NF-κB-luciferase reporter. As shown in Fig. 2B, BA-UBI also inhibited the NF-κB pathway in a dose dependent manner in these cells (IC_{50} = 21 ± 4 μM). Similar IC_{50} values of the unlabeled A-UBI were obtained using commercial NF-κB reporter Jurkat T cells (NF-κB-bla Jurkat CellSensor cell line, Invitrogen) following stimulation with TNF-α, PMA/ionomycin, and CD3/CD28, whilst no NF-κB inhibition was observed with A-NOA or A-NOA-LZ^{PP} (data not shown). To determine the inhibition mechanism of UBI in the NF-κB pathway, we assessed whether A-UBI affects nuclear translocation of endogenous p65 as well as IKK activation. As shown in Fig. 3A, p65 translocation was strongly blocked in the presence of A-UBI in pre-B cells 70Z/3 stimulated with LPS. However, no impairment of p65 translocation was observed in the presence of the NOA peptide control. Incubation of 70Z/3 with A-UBI showed a marked reduction of IKK activity in response to LPS (Fig. 3B), indicating that the inhibitory effect of UBI occurs at the level of the IKK complex. These results demonstrated that the NEMO-derived UBI peptide is a new inhibitor of the NF-κB pathway and acts in different cell types in response to a wide variety of NF-κB signals.

We next assessed whether the inhibitory effects of UBI are specific to the NF-κB pathway by measuring the effect of UBI on other signal transduction pathways. These included the mitogen-activated protein kinase (MAPK) and nuclear factor of activated T cells (NFAT) pathways. Jurkat T cells were transiently transfected with different luciferase reporter plasmids to measure activation of the MAPK/ERK, MAPK/JNK, NF-κB and NFAT pathways. The reporter plasmids used were SRE-luc, AP1-luc, Igκ-luc and NFAT-luc, respectively. The Serum Response Elements (SRE) bind Serum-Response Factor (SRF) and recruit ternary complex factors such as Elk-1. Elk-1 is phosphorylated by ERKs (also JNK and p38 isoforms [47]), whereas the AP-1 transcription factor and its major component c-Jun are mostly activated by JNKs [48]. The NFAT transcription factors are targets of the calcium/calmodulin-dependent phosphatase calcineurin which is activated by an increase of intracellular Ca^{2+} concomitent with T-cell receptor activation [49]. Fig. 4 shows that the stimulation of Jurkat cells with PMA (100 ng/ml) and ionomycin (1 μg/ml) induces transcriptional activation of these different luciferase reporters. All of these transcriptional activations were almost unchanged in the presence of 5 μM of BA-NOA and BA-UBI, whereas a significant NF-κB inhibition was specifically observed with BA-UBI (41%). This indicates that the MAPK and NFAT pathways do not appear to be affected by UBI as judged by gene reporter assays. Determination of kinase activity is generally considered to be more sensitive than gene reporter assay. We also examined LPS-induced p38 and JNK activation in pre-B lymphocytes since A-UBI inhibits the LPS-induced IKK activation in these cells. As LPS was a poor activator of JNK1 in this 70Z/3 cell line, we were not able to examine JNK1 activation. Neither A-UBI nor A-NOA inhibits JNK2 or p38

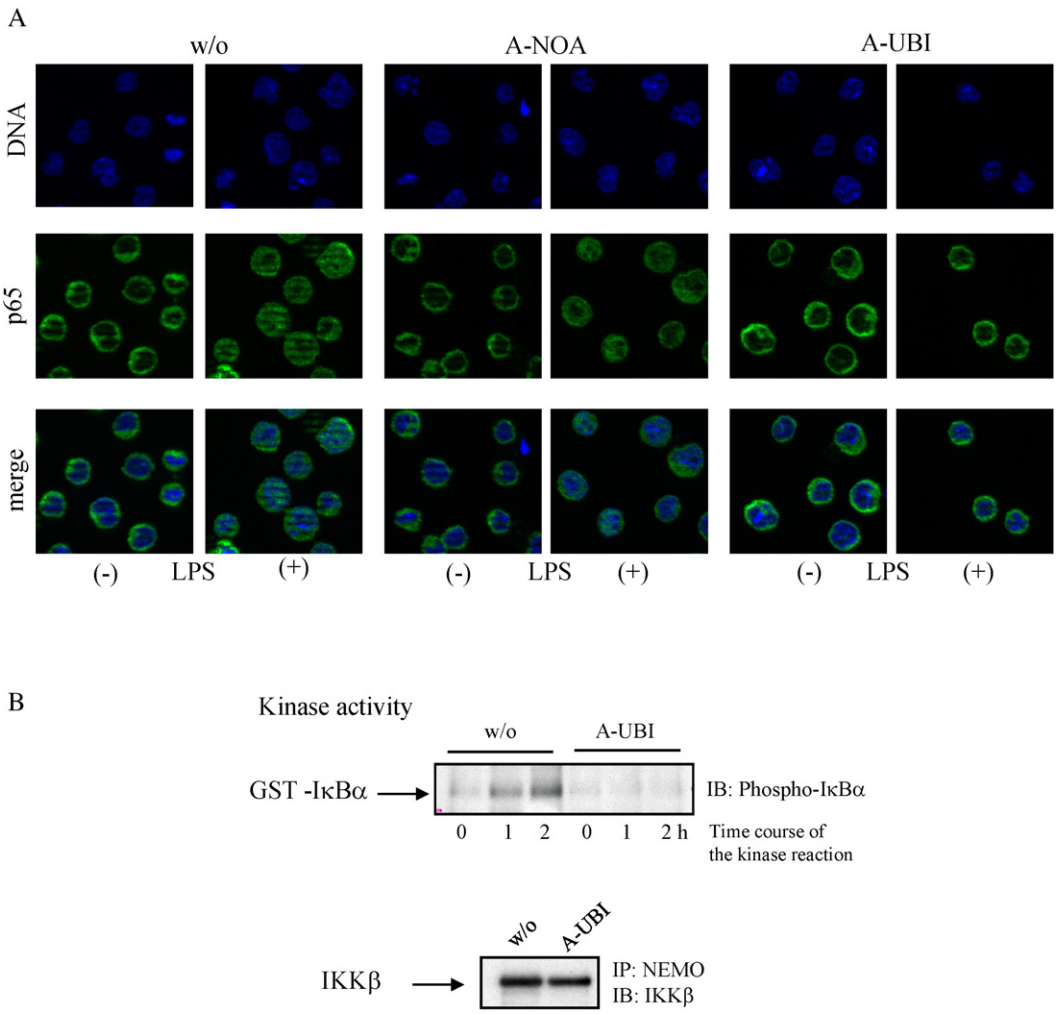

Fig. 3. UBI peptide inhibits the nuclear translocation of NF-κB p65 and the IKK kinase activity. (A) 70Z/3 cells were stimulated or not with LPS for 2 h without peptide (w/o), either with A-UBI or with the control A-NOA (10 μM). Indirect immunofluorescence assays were performed on fixed cells as described in Section 2. p65 localization in the cells is visualized with the anti-p65 primary antibody and the secondary antibody, Alexa-488 coupled goat anti-mouse IgG. DAPI was used as a nuclear stain and merged with p65 staining. (B) Pre-B lymphocytes 70Z/3 stimulated with LPS for 40 min were incubated without or with A-UBI peptide (10 μM). Following immunoprecipitation of the IKK complex with anti-NEMO antibody, the level of IKKβ was determined with an anti-IKKβ mouse monoclonal antibody (lower panel). Kinase activity was measured using GST-IκBα as substrate and an antibody against phospho-IκBα to detect the reaction product.

activation (Fig. S2). On the other hand a significant increase of JNK2 activity was observed with A-UBI compared to A-NOA. This JNK activation may be indirect and may result from an inhibition of the NF-κB pathway as previously shown with cells deficient of either RelA (p65) or NEMO [50]. We conclude that UBI targets a protein which is specifically involved in the activation of the NF-κB pathway.

3.2. BA-UBI peptide binds in vitro to the CC2-LZ domain of NEMO

Unlike NOA-LZ [20], UBI and NOA are unable to self-associate. Indeed, gel filtration experiments showed that NOA and UBI do not form oligomeric coiled-coil structures since both peptides behave as monomers at concentrations up to 100 μM (data not shown). Moreover, CD spectra of UBI and NOA revealed low α-helical contents of 24% and 14%, respectively (Fig. S3), which remains unchanged when varying peptide concentration from 20 μM to 200 μM. Taking into account the structure of CC2-LZ, the slight but significant gain of α-helical content for the UBI peptide is consistent with the formation of i and $i+4$ ionic interactions between the R304 and E308 side chains (see Section 4). Fluorescence polarization experiments show that BA-UBI specifically binds to the CC2-LZ domain of NEMO. UBI forms a stable CC2-LZ/peptide complex with a dissociation constant of 17 ± 8 μM (Fig. 5A). In comparison, the BA-NOA and BA peptides display less affinity with K_D values of 192 ± 15 μM and 426 ± 35 μM, respectively (Fig. 5A). This interaction does not depend on the CPP sequence because the poly R_7 peptide (BR_7-UBI) displays a similar dissociation constant (Fig. 5B).

Using various peptides that mimic the CC2 (residues 248–287) and NOA-LZ (residues 294–336), competition assays were performed to locate the binding site of UBI (Fig. 5C). Increasing the concentration of R_7-NOA-LZ competed with the binding of BA-UBI to the CC2-LZ domain whereas no significant competition was observed with CC2. The defective dimeric mutant, R_7-NOA-LZ^{PP}, was used as a control to verify the specificity of the binding (Fig. 5C). This control peptide is a less efficient competitor than R_7-NOA-LZ, since its IC_{50} value was 10.5-fold higher. We conclude that UBI specifically interacts in vitro with the NOA-LZ region of NEMO.

3.3. UBI directly interacts with the full length NEMO in cells

To determine whether inhibition of NF-κB activity by UBI was due to a direct interaction with NEMO, we synthesized biotinylated

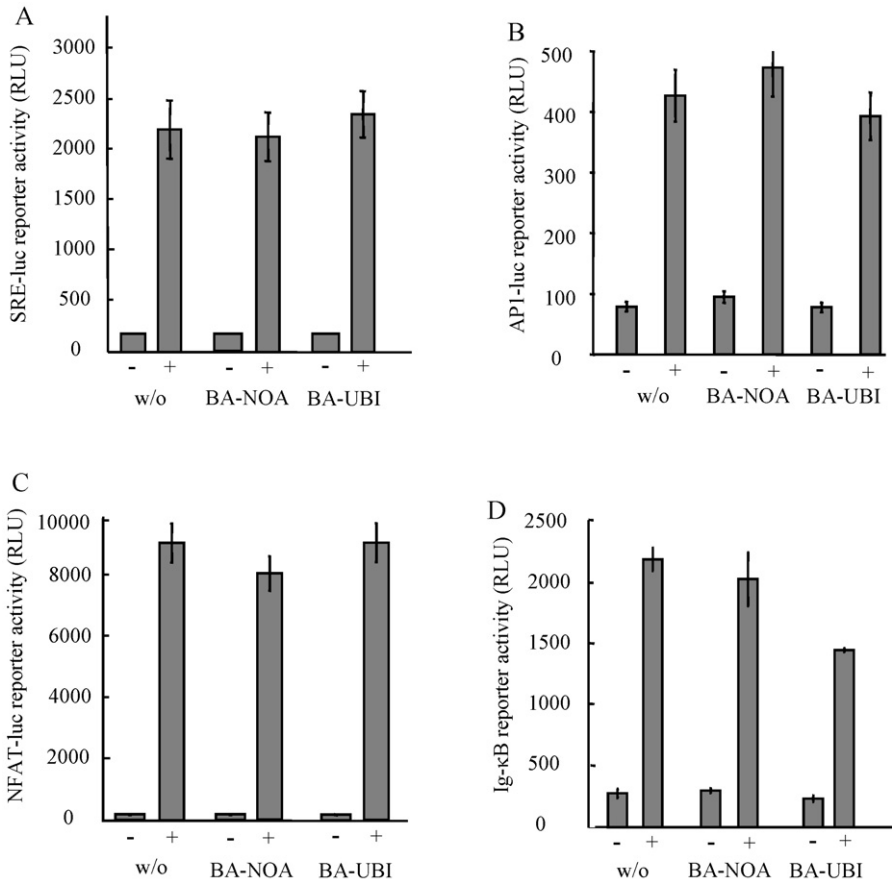

Fig. 4. UBI does not significantly affect other signaling pathways. Effect of BA-NOA and BA-UBI on the MAPK/ERK, MAPK/JNK, NFAT and NFκ-B pathways in T lymphocytes. Jurkat cells were transiently transfected with different reporter plasmids, SRE-luc A, AP1-luc B, NFAT-luc C, Igκ-luc D, and then incubated with or without (w/o) the indicated peptides (5 μM) for 2 h. Cells were then mock-stimulated (−) or stimulated (+) with PMA (100 ng/ml) and ionomycin (1 μg/ml) for 5 h. Mean values (±SD) from two separate experiments are shown.

BioA-UBI and BioA-NOA (Table S1). After 2 h incubation with BioA-UBI or BioA-NOA peptide (10 μM), 70Z/3 cells were extensively washed to remove any excess peptide contained in the extracellular media. Following cell lysis, we then performed pull-down experiments with neutravidin beads, and examined by Western blotting the intracellular proteins bound to biotinylated peptides. A specific interaction of the BioA-UBI was found with NEMO, whereas no association was observed with either BioA-NOA or with neutravidin beads alone (Fig. 6, upper left panel). This interaction was specific since the RIP1 or glyceraldehyde 3-phosphate dehydrogenase (GAPDH) protein was not able to bind any biotinylated peptides (Fig. 6, right panel). This specificity appears to be high since BioA-UBI displays a weaker binding to NRP/optineurin which also contains the NOA UBD (Fig. 6, lower left panel) [22,23]. A reverse and specific interaction of NEMO was also observed with the fluorescent BA-UBI peptide (Table S1) when we pulled-down Flag-NEMO from NEMO-deficient T lymphocytes stably reconstituted with a Flag version of NEMO (Fig. S4). Altogether, our results show that the BA-UBI specifically binds to NEMO in cells, with a perfect correlation between the effect on the inhibition of the NF-κB pathway and its ability to interact with NEMO.

3.4. UBI does not interfere with NEMO oligomerization

To analyze the molecular mechanism of the inhibition of NF-κB following treatment with UBI, we set up an assay to probe the oligomerization state of NEMO. For this, we used two plasmids expressing both GFP-NEMO and Flag-NEMO fusion proteins. The plasmids were co-transfected into HEK 293T cells to over-express exogenous GFP-NEMO and Flag-NEMO fusion proteins thereby enforcing oligomerization of NEMO. Following detergent lysis, Flag-NEMO proteins were immunopurified using anti-Flag agarose beads. The fluorescence associated with the beads was due to an association of Flag-NEMO with GFP-NEMO subunits within hetero-oligomers. This allowed us to estimate the amount of oligomers (dimer and higher order oligomers) present in the cellular extracts. Controls including the expression of GFP-NEMO alone or the co-expression of Flag-NEMO and GFP proteins did not show any fluorescence associated with the anti-Flag beads (Fig. 7A).

To validate this fluorescence-based assay, we used the first generation A-NOA-LZ peptide as a positive control. This peptide was shown to inhibit in vitro CC2-LZ oligomerization of NEMO [20]. As shown in Fig. 7B, incubation with A-NOA-LZ (20 μM) strongly reduces the amount of fluorescent NEMO subunit, indicating that the A-NOA-LZ peptide inhibits NEMO oligomerization in cells. This decrease was not due to a decrease of the Flag-NEMO immobilized on beads since immunoblots showed similar amounts of Flag-NEMO in all transfected samples (Fig. 7B). An important negative control was also provided by the defective dimeric mutant (A-NOA-LZ^{PP}), which had a double mutation within the dimerization core of the C-terminal half of NOA-LZ.

Using this cell based assay, we examined the capacity of the A-UBI peptide to alter oligomerization of NEMO. As with A-NOA-LZ^{PP}, A-UBI and A-NOA (20 μM) did not affect the amount of NEMO oligomers in the cells. Despite the ability of UBI to bind with the

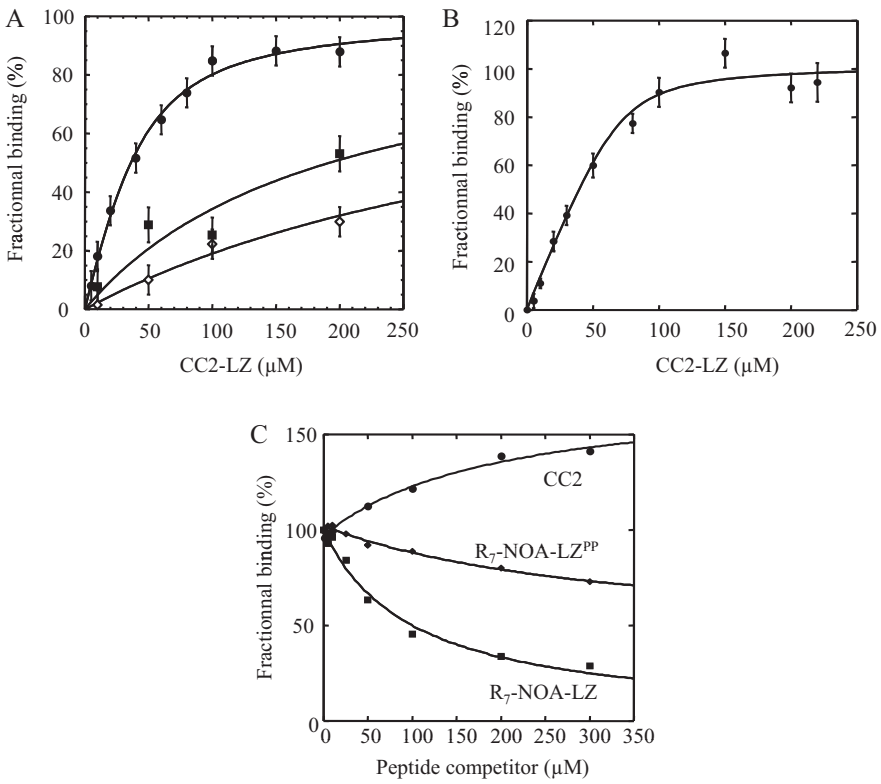

Fig. 5. In vitro binding of BA-UBI to the CC2-LZ. (A) Fluorescently labelled BA (open losanges), BA-NOA (filled squares), or BA-UBI (filled circles) (10 μM) were incubated with increasing concentrations of CC2-LZ and the complex formation was monitored by fluorescence polarization. Data were fitted to the binding isotherm equation indicating an association constant between CC2-LZ and BA-UBI with a K_D = 17 μM. (B) The same experiment was performed with BR_7-UBI (10 μM), providing a similar association constant (K_D = 21 μM). (C) Fluorescent BA-UBI (10 μM) was incubated with CC2-LZ (30 μM) to pre-form the peptide:protein complex. Increasing concentrations of R_7-NOA-LZ (filled squares), CC2 (filled circles), and R_7-NOA-LZ^{PP} (filled losanges) were then added to compete the binding of BA-UBI to CC2-LZ. Mean values (±SD) correspond to 20 measurements taken over a 2-min period.

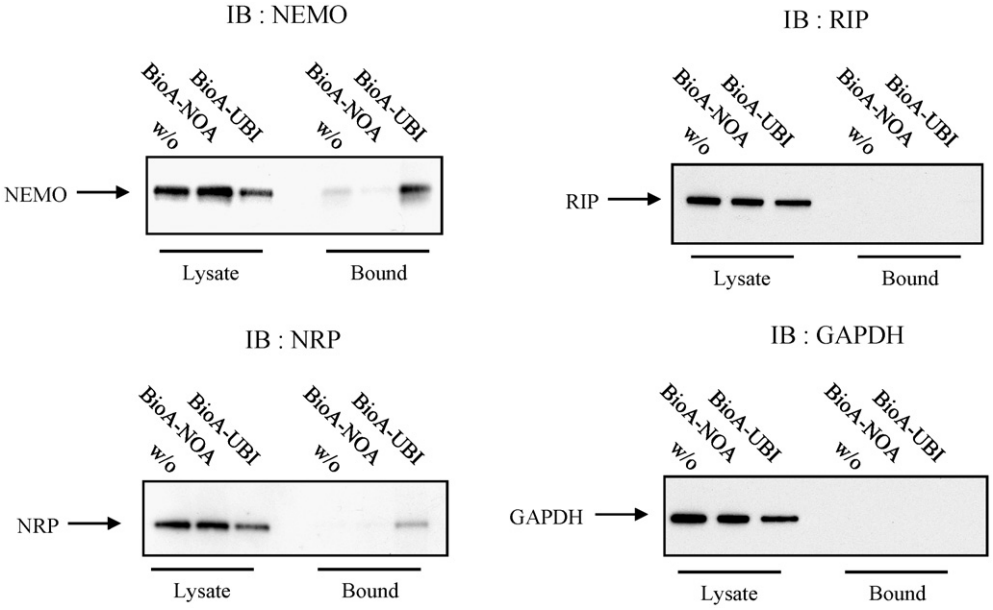

Fig. 6. Specific inhibition of NF-κB activation occurs through targeting endogenous NEMO. 70Z/3 cells were incubated for 2 h without (w/o) or with 10 μM indicated biotinylated peptides (BioA-NOA and BioA-UBI). Identification of lysates (10%) or bound proteins in pull-down experiments were performed by immunoblotting (IB) with the indicated antibodies.

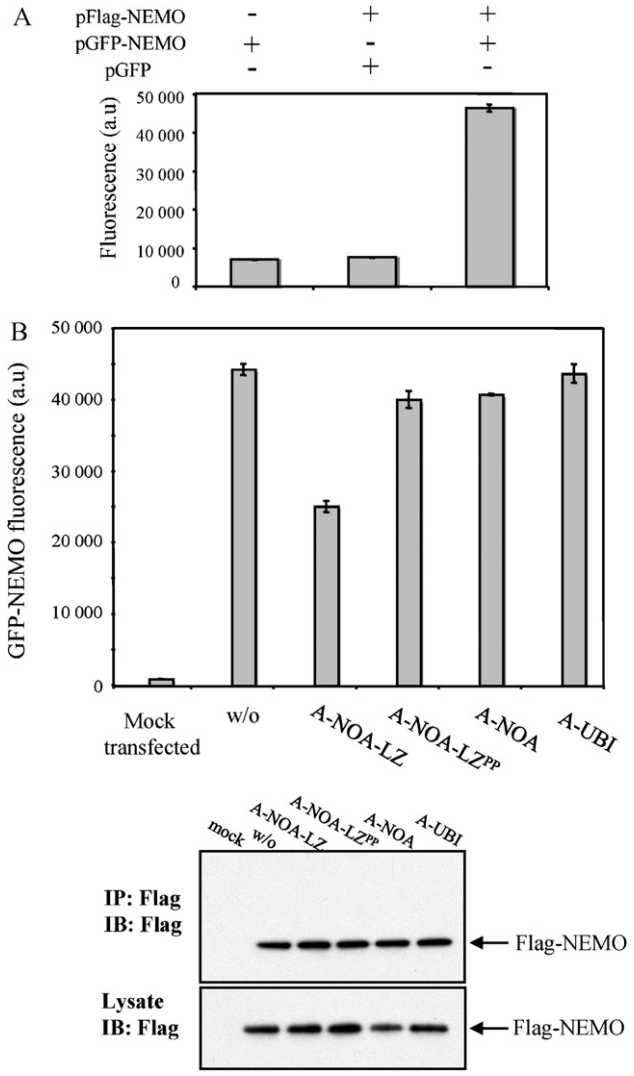

Fig. 7. UBI peptide does not inhibit NEMO oligomerization. (A) HEK 293T cells were transfected with pGFP, pGFP-NEMO, and pFlag-NEMO. The whole cell lysates were subjected to Flag-NEMO immunoprecipitation with anti-Flag beads. After several washes under stringent conditions, GFP-NEMO bound to the beads was determined by fluorescence. (B) HEK 293T cells co-transfected with pGFP-NEMO and pFlag-NEMO were treated for 2 h with the indicated peptides at 20 μM. The NEMO hetero-oligomers were then immunopurified using anti-Flag beads and the amount of the GFP-NEMO subunit bound to hetero-oligomers was examined by fluorescence. Whole cell lysates and the amount of Flag-NEMO associated with the anti-Flag beads were also analyzed by immunoblotting with the anti-Flag antibody.

NOA-LZ domain of NEMO, we conclude that NF-κB inhibition by UBI results from a mechanism that is independent of the state of oligomerization of NEMO within the cell.

3.5. UBI inhibits the interaction between NOA-containing CC2-LZ and polyubiquitin chains

NEMO is now recognized as an important sensor of K63-linked and linear polyubiquitin chains [9,24,25,27]. To determine whether UBI affects the interaction between NEMO and poly-ubiquitin chains, we developed an assay that used the NOA/UBAN UBD of the CC2-LZ domain of NEMO as a bait to pull down the polyubiquitin chains (free and anchored polyubiquitin chains). To this end, biotinylated-CC2-LZ (10 μg) coated onto magnetic beads was pre-incubated with A-NOA or A-UBI peptides (20 μM). Crude extracts from NEMO-deficient T lymphocytes stimulated or not with TNF-α were then added to this mix. After extensive washing of beads, the polyubiquitin chains bound to CC2-LZ were analyzed by Western blotting using anti-ubiquitin antibody. Consistent with previous studies [24,25], cell stimulation resulted in a strong increase of polyubiquitin chains linked to the NOA UBD of CC2-LZ in a TNF-α dependent manner. As shown in Fig. 8A, the A-UBI peptide impairs the interaction of CC2-LZ with the polyubiquitin chains formed after stimulation with TNF-α. In contrast, no inhibition was observed in the absence of peptide or in the presence of the A-NOA peptide. We then tried to determine whether the UBI peptide preferentially competes with ubiquitin for binding to CC2-LZ and whether the competition effect depends on one type of ubiquitin-linkage (K63 or linear). To this end, we

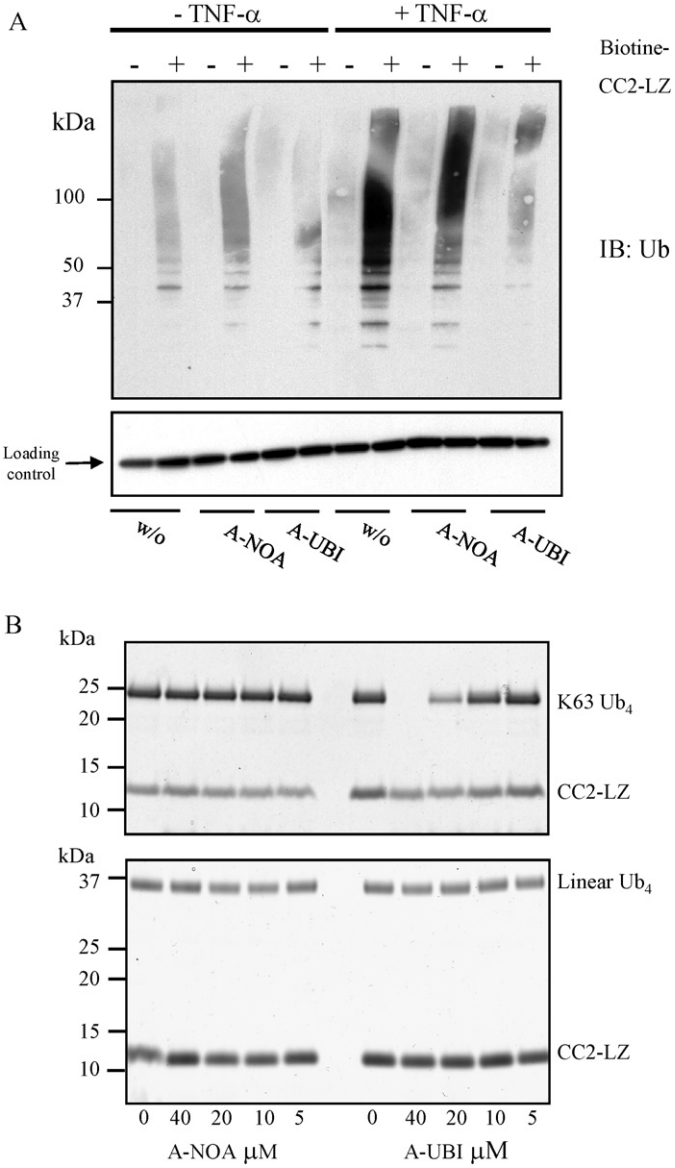

Fig. 8. Interaction of UBI with NEMO prevents the binding of polyubiquitin chains to the CC2-LZ domain. (A) Cytosolic extracts stimulated (+TNF-α) or not (−TNF-α) with 10 ng/ml TNF-α were incubated with (+) or without (−) biotinylated CC2-LZ coated on beads and with indicated peptides (20 μM). The amount of polyubiquitinated proteins bound to the beads was determined by immunoblotting with anti-ubiquitin antibody. Loading control was determined with the NDP-kinase antibody. (B) His-CC2-LZ (4 μM) coated beads were incubated with 2 μM of K63-linked (upper panel) or linear (lower panel) tetraubiquitin and an increasing concentration (0–40 μM) of A-UBI and A-NOA peptides for 1 h at room temperature. The tetraubiquitin bound to CC2-LZ beads was determined by Coomassie blue staining.

first compared the ubiquitin binding properties of BA-UBI and BA-NOA peptides by fluorescence polarization. The BA-NOA peptide alone is able to bind to K63-linked triubiquitin in a cooperative manner with an affinity of 90 ± 6 μM and a Hill coefficient (n_H) of 4 (Fig. S5). In contrast, the affinity of BA-UBI is significantly reduced (3.6-fold) and no ubiquitin binding cooperativity is observed (n_H = 1), confirming that the single Asp to Arg mutation in UBI impairs ubiquitin binding. For competition assays, in vitro pull down experiments were performed with His-tagged CC2-LZ (4 μM) coated on Ni-NTA beads and incubated with 2 μM K63-linked or linear tetraubiquitin with a variable concentration (0–40 μM) of A-UBI or A-NOA peptide. After washing the beads, the CC2-LZ complex with tetraubiquitin was revealed by SDS-PAGE following Coomassie blue staining. As shown in Fig. 8B, the A-UBI peptide, but not the A-NOA peptide, competes efficiently in a dose-dependent manner with K63-linked tetraubiquitin for binding to CC2-LZ, whilst no competition was observed with the linear tetraubiquitin in the presence of A-NOA or A-UBI peptides. We therefore conclude that the mechanism of NF-κB inhibition by UBI results from the binding of UBI to the NOA-LZ domain that preferentially impairs the interaction between NEMO and K63-linked polyubiquitin chains.

4. Discussion

Developing a specific protein-protein interaction inhibitor is still a challenging task, despite the great advances that have been made in this field over the last decade. In particular, there has been considerable success in developing short peptide inhibitors that recapitulate the sequence of the key strand or helix that mediates binding [51–54]. In the present study, we designed a new peptide inhibitor that derived from the NOA/UBAN ubiquitin binding site of NEMO. This peptide inhibits the NF-κB pathway at the IKK level (Fig. 3B) by binding to the NOA-LZ region of NEMO (Fig. 5C). We demonstrated that the peptide inhibition occurs by targeting NEMO in cells (Fig. 6) and by preventing the interaction between the NOA containing CC2-LZ domain of NEMO and free or anchored polyubiquitin chains (Fig. 8A). This is consistent with previous studies since UBI lacks the D304 binding determinant which is a "hot spot" residue in the binding interface between NOA UBD and polyubiquitins [25–27,38,55]. However, it is surprising not to observe any marked inhibition of the NF-κB pathway with the cell-permeable NOA peptide. Indeed, this peptide could compete with the NOA-containing CC2-LZ in polyubiquitin chain binding and therefore could act as a potent NF-κB inhibitor. The lack of inhibition is not due to the inappropriate sequence of the NOA UBD for two reasons. First, the NOA peptide (residues 294–314) encompasses most of determinants which make specific contacts with the distal ubiquitin in the crystal complex with a K63-linked [28] or linear diubiquitin chain [27]. Second, longer NOA peptides with an extension at N-terminus (residues 293–314) or C-terminus (residues 294–322) do not inhibit the NF-κB activation (data not shown). A possible explanation could be in the improved binding affinity of UBI for NEMO relative to the NOA peptide (11-fold, Fig. 5A and B). The inhibition of UBI may therefore result from a dual effect of the D304R mutation in the NOA peptide. First, the mutation markedly increases the helical character of the peptide (Fig. S3) which consequently promotes binding to CC2-LZ (Fig. 5) or the full length NEMO in cells (Fig. 6), possibly by reducing the entropy cost of binding. Second, the mutation prevents the formation of a stable complex with ubiquitin once UBI is bound to the NOA region of NEMO through hetero-oligomeric interactions.

Structural modeling of the mutation did not reveal any new interhelical interactions in the native dimeric structure of the CC2-LZ coiled-coil (PDB 2V4H) that could explain this gain of affinity. In contrast, R304 could make more favorable intrahelical interactions with E308 at i + 4 in the monomer helix through formation of a salt bridge. This observation is supported by CD experiments which showed that the gain of helicity from 14% to 24% relative to the NOA peptide is compatible with the stabilization of one α-helical turn (Fig. S3). Contrary to the general behavior of the coiled-coil peptides [56,57], this gain of the helix formation is not due to peptide dimerization. This was seen from the lack of concentration dependence of CD spectra as well as size exclusion chromatography at different peptide concentrations (data not shown). Recent consensus holds that coiled-coil formation can be promoted through "trigger sequences" which encode stable monomeric α-helices [58–60]. We therefore hypothesize that R304 may behave as "trigger site" in which coiled-coil interaction with CC2-LZ is promoted through the binding of UBI monomer having preformed α-helix. This is similar to the GCN4 leucine zipper whose coiled-coil folding is enhanced through an intramolecular salt bridge within the trigger sequence [60].

Given the complexities of transcriptional NF-κB responses, it is impossible to conclusively rule out any off target activity by UBI. However, in different murine and human cell types, inhibition of NEMO dependent NF-κB activation in response to a broad range of NF-κB signal (LPS, PMA/iono, TNF and IL1) correlates strongly with the binding to NEMO in cells. This binding appears to be specific since UBI exhibits (i) no interaction with GAPDH and RIP and (ii) a weaker binding with NRP/optineurin although this latter protein shares a similar NOA UBD with NEMO. Furthermore, in this context, there is no inhibitory effect of UBI in MAPK pathways as determined by gene reporter assays or p38 and JNK2 kinases activities. It is therefore clear that endogenous NEMO is likely the main target of UBI.

The current consensus is that the binding of NEMO to polyubiquitin chains is a key event for IKK activation. However, it is currently unclear which type of ubiquitin-linkage is predominantly required for IKK activation. In particular, for the TNF-α pathway there are conflicting results regarding the involvement of linear [9], K63-linked [61,62], or mixed (both K63 and K48 [14]) polyubiquitin chains in the activation of IKK. The controversy mainly arises from the difficulty to identify the predominant ubiquitin-linkage. This is because several sets of ubiquitination enzymes (E2 and E3) appear to be involved in one type of ubiquitin-linkage and are recruited to TNF-α receptor signaling complexes in a ligand dependent manner. The ubiquitination enzymes include the LUBAC complex, which synthesize linear ubiquitin chains [9,13,27], the cIAP1/2:UbcH5 complex [14], which mediates polymerization of both K48-and K63-linked chains, and the TRAF2:Ubc13-Uev1a complex which specifically generates either free [63] or anchored K63-linked chains when bound to cIAP1/2 [61,64,65]. Furthermore, the synthesis of K63-linked chains is not only restricted to Ubc13 as the loss of its gene can be compensated by other E2 and E3 enzymes such as UbcH5 or cIAP1/2 [14,62,66]. However, in the IL-1 receptor pathway, a predominant role of K63-linked chains has been clearly demonstrated using a ubiquitin-replacement strategy and RNAi-mediated knockdown of endogenous ubiquitin [14]. In the present study, we developed a novel NEMO inhibitor that inhibited both the IL-1 and TNF-α pathways by preventing the interaction between the NOA UBD of NEMO and polyubiquitin chains. Similar experiments depicted in Fig. 8A were performed with the full length NEMO, which contains the two NOA and ZF UDBs (also called NOAZ domain). We were unable to detect a significant impairment of the interaction between polyubiquitin chains and NEMO with A-UBI, possibly due to the important contribution of the second UBD formed by the NEMO ZF in the overall interaction with polyubiquitin chains (not shown). Given that UBI solely blocks the NOA binding site to ubiquitin (Fig. 8A), this suggests that both ubiquitin binding sites of NEMO should be simultaneously

occupied by ubiquitin units to fully preserve the NEMO function. The presence of NEMO ZF may also explain why no complete inhibition of NF-κB activation was observed at a saturating concentration of UBI (Fig. 2A and B). The residual NF-κB activity indeed could result from the ZF UBD of NEMO, which likely maintains a residual ubiquitin binding activity of NEMO in the cells.

Remarkably, in vitro pull-down experiments showed that A-UBI, but not A-NOA, competes with K63-linked tetraubiquitin for binding to CC2-LZ. On the other hand, no competition was observed between linear-tetraubiquitin and A-NOA or A-UBI peptides (Fig. 8B). This is consistent with previous reports of structural complexes of the NOA UBD domain with linear [27] and K63-linked diubiquitin [28]. Indeed, the amino acid sequence of UBI (residues 294–314) recapitulates all binding determinants for K63-linked chains but partially lacks those for linear chains. In particular, the E317 and E320 binding determinants for the proximal ubiquitin moiety of linear diubiquitin [27] are missing. Therefore, we believe that the predominant type of ubiquitin-linkage that is critical for signal-induced IKK activation via NEMO binding is likely to consist of K63-linked chains, or mixed chains containing specific K63-linkage. This is because UBI only disrupts the binding to K63-linked tetraubiquitin chains. Nevertheless, our data do not rule out the possibility that the LUBAC-generated linear chains are required for full NF-κB activation. Indeed, LUBAC recruitment to the receptor also appears to be mediated by homogenous or mixed K63-linked chains [13]. This leads in general to the linear ubiquitinylation and stabilization of the receptor signaling complexes such as TNF-R1 or CD40L-R [10]. Thus, these LUBAC-generated linear chains may serve as a downstream amplification signal for enhancing NEMO recruitment and ultimately increasing the activation of IKK and NF-κB. Further studies are required to clearly elucidate the mechanism(s) by which linear and K63-linked chains trigger the IKK activation in the vinicity of various receptor complexes. In any case, it appears that the identification of the new NEMO inhibitor such as UBI would be helpful for elucidating the role of different ubiquitin-linkages on IKK-induced NF-κB activation in inflammation and cancer.

Acknowledgements

We thank A. Israël for fruitful discussions; P. England and B. Baron from the Plate-Forme de Biophysique des Macromolécules et de leurs Interactions, E. Laplantine for his help in immunofluorescence microscopy, M.M. Mhlanga and S. Levy for critical reading of the manuscript, and S.C. Sun (Houston, USA) for JM4.5.2 cells. We are indebted to F. Traincard for providing lentiviruses containing a NF-κB reporter luciferase gene. This work was supported in part by grants from the Cancéropôle Ile-de-France, the BNP-Paribas Foundation, and the Institut de Recherches Servier.

Appendix A. Supplementary data

Supplementary data associated with this article can be found, in the online version, at doi:10.1016/j.bcp.2011.07.083.

References

[1] Hayden MS, Ghosh S. Shared principles in NF-kappaB signaling. Cell 2008;132:344–62.
[2] Perkins ND. Integrating cell-signalling pathways with NF-kappaB and IKK function. Nat Rev Mol Cell Biol 2007;8:49–62.
[3] Scheidereit C. IkappaB kinase complexes: gateways to NF-kappaB activation and transcription. Oncogene 2006;25:6685–705.
[4] Vallabhapurapu S, Karin M. Regulation and function of NF-kappaB transcription factors in the immune system. Annu Rev Immunol 2009;27:693–733.
[5] Sato S, Sanjo H, Takeda K, Ninomiya-Tsuji J, Yamamoto M, Kawai T, et al. Essential function for the kinase TAK1 in innate and adaptive immune responses. Nat Immunol 2005;6:1087–95.
[6] Shim JH, Xiao C, Paschal AE, Bailey ST, Rao P, Hayden MS, et al. TAK1, but not TAB1 or TAB2, plays an essential role in multiple signaling pathways in vivo. Genes Dev 2005;19:2668–81.
[7] Kulathu Y, Akutsu M, Bremm A, Hofmann K, Komander D. Two-sided ubiquitin binding explains specificity of the TAB2 NZF domain. Nat Struct Mol Biol 2009;16:1328–30.
[8] Sato Y, Yoshikawa A, Mimura H, Yamashita M, Yamagata A, Fukai S. Structural basis for specific recognition of Lys 63-linked polyubiquitin chains by tandem UIMs of RAP80. EMBO J 2009;28:2461–8.
[9] Tokunaga F, Sakata S, Saeki Y, Satomi Y, Kirisako T, Kamei K, et al. Involvement of linear polyubiquitylation of NEMO in NF-kappaB activation. Nat Cell Biol 2009;11:123–32.
[10] Gerlach B, Cordier SM, Schmukle AC, Emmerich CH, Rieser E, Haas TL, et al. Linear ubiquitination prevents inflammation and regulates immune signalling. Nature 2011;471:591–6.
[11] Ikeda F, Deribe YL, Skanland SS, Stieglitz B, Grabbe C, Franz-Wachtel M, et al. SHARPIN forms a linear ubiquitin ligase complex regulating NF-kappaB activity and apoptosis. Nature 2011;471:637–41.
[12] Tokunaga F, Nakagawa T, Nakahara M, Saeki Y, Taniguchi M, Sakata S, et al. SHARPIN is a component of the NF-kappaB-activating linear ubiquitin chain assembly complex. Nature 2011;471:633–6.
[13] Haas TL, Emmerich CH, Gerlach B, Schmukle AC, Cordier SM, Rieser E, et al. Recruitment of the linear ubiquitin chain assembly complex stabilizes the TNF-R1 signaling complex and is required for TNF-mediated gene induction. Mol Cell 2009;36:831–44.
[14] Xu M, Skaug B, Zeng W, Chen ZJ. A ubiquitin replacement strategy in human cells reveals distinct mechanisms of IKK activation by TNFalpha and IL-1beta. Mol Cell 2009;36:302–14.
[15] Xia ZP, Sun L, Chen X, Pineda G, Jiang X, Adhikari A, et al. Direct activation of protein kinases by unanchored polyubiquitin chains. Nature 2009;461:114–9.
[16] Marienfeld RB, Palkowitsch L, Ghosh S. Dimerization of the I kappa B kinase-binding domain of NEMO is required for tumor necrosis factor alpha-induced NF-kappa B activity. Mol Cell Biol 2006;26:9209–19.
[17] Rushe M, Silvian L, Bixler S, Chen LL, Cheung A, Bowes S, et al. Structure of a NEMO/IKK-associating domain reveals architecture of the interaction site. Structure 2008;16:798–808.
[18] Bagneris C, Ageichik AV, Cronin N, Wallace B, Collins M, Boshoff C, et al. Crystal structure of a vFlip-IKKgamma complex: insights into viral activation of the IKK signalosome. Mol Cell 2008;30:620–31.
[19] Grubisha O, Kaminska M, Duquerroy S, Fontan E, Cordier F, Haouz A, et al. DARPin-assisted crystallography of the CC2-LZ domain of NEMO reveals a coupling between dimerization and ubiquitin binding. J Mol Biol 2010;395:89–104.
[20] Agou F, Courtois G, Chiaravalli J, Baleux F, Coic YM, Traincard F, et al. Inhibition of NF-kappa B activation by peptides targeting NF-kappa B essential modulator (nemo) oligomerization. J Biol Chem 2004;279:54248–57.
[21] Heyninck K, Kreike MM, Beyaert R. Structure-function analysis of the A20-binding inhibitor of NF-kappa B activation, ABIN-1. FEBS Lett 2003;536:135–40.
[22] Sebban H, Yamaoka S, Courtois G. Posttranslational modifications of NEMO and its partners in NF-kappaB signaling. Trends Cell Biol 2006;16:569–77.
[23] Wagner S, Carpentier I, Rogov V, Kreike M, Ikeda F, Lohr F, et al. Ubiquitin binding mediates the NF-kappaB inhibitory potential of ABIN proteins. Oncogene 2008;27:3739–45.
[24] Ea CK, Deng L, Xia ZP, Pineda G, Chen ZJ. Activation of IKK by TNFalpha requires site-specific ubiquitination of RIP1 and polyubiquitin binding by NEMO. Mol Cell 2006;22:245–57.
[25] Wu CJ, Conze DB, Li T, Srinivasula SM, Ashwell JD. Sensing of Lys 63-linked polyubiquitination by NEMO is a key event in NF-kappaB activation. Nat Cell Biol 2006;8:398–406.
[26] Lo YC, Lin SC, Rospigliosi CC, Conze DB, Wu CJ, Ashwell JD, et al. Structural basis for recognition of diubiquitins by NEMO. Mol Cell 2009;33:602–15.
[27] Rahighi S, Ikeda F, Kawasaki M, Akutsu M, Suzuki N, Kato R, et al. Specific recognition of linear ubiquitin chains by NEMO is important for NF-kappaB activation. Cell 2009;136:1098–109.
[28] Yoshikawa A, Sato Y, Yamashita M, Mimura H, Yamagata A, Fukai S. Crystal structure of the NEMO ubiquitin-binding domain in complex with Lys 63-linked di-ubiquitin. FEBS Lett 2009;583:3317–22.
[29] Cordier F, Vinolo E, Veron M, Delepierre M, Agou F. Solution structure of NEMO zinc-finger and impact of an anhidrotic ectodermal dysplasia with immunodeficiency-related point mutation. J Mol Biol 2008;377:1419–32.
[30] Cordier F, Grubisha O, Traincard F, Veron M, Delepierre M, Agou F. The zinc finger of NEMO is a functional ubiquitin-binding domain. J Biol Chem 2009;284:2902–7.
[31] Laplantine E, Fontan E, Chiaravalli J, Lopez T, Lakisic G, Veron M, et al. NEMO specifically recognizes K63-linked poly-ubiquitin chains through a new bipartite ubiquitin-binding domain. EMBO J 2009;28:2885–95.
[32] Baud V, Karin M. Is, NF-kappaB a good target for cancer therapy? Hopes and pitfalls. Nat Rev Drug Discov 2009;8:33–40.
[33] Karin M, Greten FR. NF-kappaB: linking inflammation and immunity to cancer development and progression. Nat Rev Immunol 2005;5:749–59.
[34] Kim HJ, Hawke N, Baldwin AS, NF-kappaB. IKK as therapeutic targets in cancer. Cell Death Differ 2006;13:738–47.

[35] Legarda-Addison D, Hase H, O'Donnell MA, Ting AT. NEMO/IKKgamma regulates an early NF-kappaB-independent cell-death checkpoint during TNF signaling. Cell Death Differ 2009;16:1279–88.
[36] Nagashima K, Sasseville VG, Wen D, Bielecki A, Yang H, Simpson C, et al. Rapid TNFR1-dependent lymphocyte depletion in vivo with a selective chemical inhibitor of IKKbeta. Blood 2006;107:4266–73.
[37] Doffinger R, Smahi A, Bessia C, Geissmann F, Feinberg J, Durandy A, et al. X-linked anhidrotic ectodermal dysplasia with immunodeficiency is caused by impaired NF-kappaB signaling. Nat Genet 2001;27:277–85.
[38] Bloor S, Ryzhakov G, Wagner S, Butler PJ, Smith DL, Krumbach R, et al. Signal processing by its coil zipper domain activates IKK gamma. Proc Natl Acad Sci USA 2008;105:1279–84.
[39] Harhaj EW, Good L, Xiao G, Uhlik M, Cvijic ME, Rivera-Walsh I, et al. Somatic mutagenesis studies of NF-kappa B signaling in human T cells: evidence for an essential role of IKK gamma in NF-kappa B activation by T-cell costimulatory signals and HTLV-I Tax protein. Oncogene 2000;19:1448–56.
[40] Fontan E, Traincard F, Levy SG, Yamaoka S, Veron M, Agou F. NEMO oligomerization in the dynamic assembly of the IkappaB kinase core complex. FEBS J 2007;274:2540–51.
[41] Mousson F, Coic YM, Baleux F, Beswick V, Sanson A, Neumann JM. Deciphering the role of individual acyl chains in the interaction network between phosphatidylserines and a single-spanning membrane protein. Biochemistry 2002;41:13611–6.
[42] Courtois G, Whiteside ST, Sibley CH, Israel A. Characterization of a mutant cell line that does not activate NF-kappaB in response to multiple stimuli. Mol Cell Biol 1997;17:1441–9.
[43] Agou F, Traincard F, Vinolo E, Courtois G, Yamaoka S, Israel A, et al. The trimerization domain of NEMO is composed of the interacting C-terminal CC2 and LZ coiled-coil subdomains. J Biol Chem 2004;279:27861–9.
[44] Wyler E, Kaminska M, Coic YM, Baleux F, Veron M, Agou F. Inhibition of NF-kappaB activation with designed ankyrin-repeat proteins targeting the ubiquitin-binding/oligomerization domain of NEMO. Protein Sci 2007;16:2013–22.
[45] Jones SW, Christison R, Bundell K, Voyce CJ, Brockbank SM, Newham P, et al. Characterisation of cell-penetrating peptide-mediated peptide delivery. Br J Pharmacol 2005;145:1093–102.
[46] Wadia JS, Dowdy SF. Transmembrane delivery of protein and peptide drugs by TAT-mediated transduction in the treatment of cancer. Adv Drug Deliv Rev 2005;57:579–96.
[47] Sharrocks AD. The ETS-domain transcription factor family. Nat Rev Mol Cell Biol 2001;2:827–37.
[48] Mechta-Grigoriou F, Gerald D, Yaniv M. The mammalian Jun proteins: redundancy and specificity. Oncogene 2001;20:2378–89.
[49] Crabtree GR, Olson EN. NFAT signaling: choreographing the social lives of cells. Cell 2002;109(Suppl.):S67–79.
[50] Papa S, Bubici C, Zazzeroni F, Pham CG, Kuntzen C, Knabb JR, et al. The NF-kappaB-mediated control of the JNK cascade in the antagonism of programmed cell death in health and disease. Cell Death Differ 2006;13:712–29.
[51] Bidwell 3rd GL, Raucher D. Therapeutic peptides for cancer therapy. Part I – peptide inhibitors of signal transduction cascades. Expert Opin Drug Deliv 2009;6:1033–47.
[52] Moellering RE, Cornejo M, Davis TN, Del Bianco C, Aster JC, Blacklow SC, et al. Direct inhibition of the NOTCH transcription factor complex. Nature 2009;462:182–8.
[53] Prive GG, Melnick A. Specific peptides for the therapeutic targeting of oncogenes. Curr Opin Genet Dev 2006;16:71–7.
[54] Raucher D, Moktan S, Massodi I, Bidwell 3rd GL. Therapeutic peptides for cancer therapy. Part II – cell cycle inhibitory peptides and apoptosis-inducing peptides. Expert Opin Drug Deliv 2009;6:1049–64.
[55] Sato Y, Yoshikawa A, Yamashita M, Yamagata A, Fukai S. Structural basis for specific recognition of Lys 63-linked polyubiquitin chains by NZF domains of TAB2 and TAB3. EMBO J 2009;28:3903–9.
[56] Acharya A, Rishi V, Vinson C. Stability of 100 homo and heterotypic coiled-coil a-a' pairs for ten amino acids (A, L, I, V, N, K, S, T, E, and R). Biochemistry 2006;45:11324–32.
[57] Grigoryan G, Keating AE. Structural specificity in coiled-coil interactions. Curr Opin Struct Biol 2008;18:477–83.
[58] Kammerer RA, Schulthess T, Landwehr R, Lustig A, Engel J, Aebi U, et al. An autonomous folding unit mediates the assembly of two-stranded coiled coils. Proc Natl Acad Sci USA 1998;95:13419–24.
[59] Myers JK, Oas TG. Reinterpretation of GCN4-p1 folding kinetics: partial helix formation precedes dimerization in coiled coil folding. J Mol Biol 1999;289:205–10.
[60] Steinmetz MO, Jelesarov I, Matousek WM, Honnappa S, Jahnke W, Missimer JH, et al. Molecular basis of coiled-coil formation. Proc Natl Acad Sci USA 2007;104:7062–7.
[61] Bertrand MJ, Milutinovic S, Dickson KM, Ho WC, Boudreault A, Durkin J, et al. cIAP1 and cIAP2 facilitate cancer cell survival by functioning as E3 ligases that promote RIP1 ubiquitination. Mol Cell 2008;30:689–700.
[62] Varfolomeev E, Goncharov T, Fedorova AV, Dynek JN, Zobel K, Deshayes K, et al. c-IAP1 and c-IAP2 are critical mediators of tumor necrosis factor alpha (TNFalpha)-induced NF-kappaB activation. J Biol Chem 2008;283:24295–9.
[63] Deng L, Wang C, Spencer E, Yang L, Braun A, You J, et al. Activation of the IkappaB kinase complex by TRAF6 requires a dimeric ubiquitin-conjugating enzyme complex and a unique polyubiquitin chain. Cell 2000;103:351–61.
[64] Yin Q, Lamothe B, Darnay BG, Wu H. Structural basis for the lack of E2 interaction in the RING domain of TRAF2. Biochemistry 2009;48:10558–67.
[65] Yin Q, Lin SC, Lamothe B, Lu M, Lo YC, Hura G, et al. E2 interaction and dimerization in the crystal structure of TRAF6. Nat Struct Mol Biol 2009;16:658–66.
[66] Park SM, Yoon JB, Lee TH. Receptor interacting protein is ubiquitinated by cellular inhibitor of apoptosis proteins (c-IAP1 and c-IAP2) in vitro. FEBS Lett 2004;566:151–6.
[67] May MJ, D'Acquisto F, Madge LA, Glockner J, Pober JS, Ghosh S. Selective inhibition of NF-kappaB activation by a peptide that blocks the interaction of NEMO with the IkappaB kinase complex. Science 2000;289:1550–4.